Atmos. Chem. Phys. Discuss., doi:10.5194/acp-2016-908, 2016
Manuscript under review for journal Atmos. Chem. Phys.
Published: 2 November 2016

Atmospheric Chemistry and Physics Discussions

Secondary ozone peaks in the troposphere over the Himalayas

Narendra Ojha[1], Andrea Pozzer[1], Dimitris Akritidis[1,2], and Jos Lelieveld[1,3]

[1]Atmospheric Chemistry Department, Max Planck Institute for Chemistry, Mainz, Germany
[2]Department of Meteorology and Climatology, School of Geology, Aristotle University of Thessaloniki, Thessaloniki, Greece
[3]Energy, Environment and Water Research Center, The Cyprus Institute, Nicosia, Cyprus

Correspondence to: Narendra Ojha (narendra.ojha@mpic.de)

Abstract. Layers with strongly enhanced ozone concentrations in the middle-upper troposphere, referred to as Secondary Ozone Peaks (SOPs), have been observed in different regions of the world. Here we use the global ECHAM5/MESSy atmospheric chemistry model (EMAC) to (i) investigate the processes causing SOPs, (ii) explore both their frequency of occurrence and seasonality, and (iii) assess their effects on the tropospheric ozone budget over the Himalayas. The vertical profiles of potential vorticity (PV) and a stratospheric ozone tracer (O_3s) in EMAC simulations, in conjunction with the structure of SOPs, suggest that SOPs over the Himalayas are formed by Stratosphere-to-Troposphere Transport (STT) of ozone. The spatial distribution of O_3s further shows that such effects are in general confined to the northern part of India. Model simulated ozone distributions and backward air trajectories show that ozone rich air masses, associated with STT, originate as far as northern Africa and the North Atlantic Ocean, the Middle-East, as well as nearby regions in Afghanistan and Pakistan, and are rapidly (within 2–3 days) transported to the Himalayas. Analysis of a 15-year (2000-2014) EMAC simulation shows that the frequency of SOPs is highest during the pre-monsoon season (e.g. 11% of the time in May), while no intense SOP events are found during the July-October period. The SOPs are estimated to enhance the Tropospheric Column Ozone (TCO) over the central Himalayas by up to 26%.

1 Introduction

Tropospheric ozone is a short-lived climate forcer (Shindell et al., 2012) and an air pollutant with adverse effects on human health and crop yields (Monks et al., 2015, and references therein). The effects of tropospheric ozone on crop yields and human health occur near the surface, whereas its radiative forcing is shown to be strongest in the middle-upper troposphere (e.g. Lacis et al., 1990;

Atmos. Chem. Phys. Discuss., doi:10.5194/acp-2016-908, 2016
Manuscript under review for journal Atmos. Chem. Phys.
Published: 2 November 2016

Atmospheric Chemistry and Physics Discussions

Myhre et al., 2013; Monks et al., 2015). The processes controlling tropospheric ozone in the middle and upper troposphere can be different from those near the surface. The photochemistry involving non-methane volatile organic compounds (NMVOCs) and carbon monoxide, in the presence of nitrogen oxides (NOx) primarily controls ozone pollution in the planetary boundary layer. In contrast, dynamics involving Stratosphere-Troposphere Exchange (STE) play a key role in the middle-upper troposphere (e. g. Holton and Lelieveld, 1996; Lelieveld and Dentener, 2000; Neu et al., 2014; Ojha et al., 2014; Monks et al., 2015). Therefore, to quantify the relative contributions of photochemical and dynamical processes to the ozone budget and assess the climatic impacts of anthropogenic ozone, studies of the vertical distribution of ozone are essential.

Ozone observations have been conducted globally and locally using different instruments and platforms as reviewed recently by Tanimoto et al. (2015). Balloon-borne observations employing ozonesondes offer the advantage of measuring ozone across the tropopause. Analyses of ozonesonde observations have provided valuable information on the variability, general features and trends in ozone profiles (e.g. Logan, 1985, 1994). Secondary maxima in ozone profiles, called Secondary Ozone Peaks (SOPs), are a unique phenomenon in which anomalously large ozone concentrations are observed in confined layers in the middle-upper troposphere or lower stratosphere.

The occurrences of SOPs, underlying processes and their global distribution have been discussed in a limited number of studies (Dobson, 1973; Reid and Vaughan, 1991; Varotsos et al., 1994), reviewed by Lemoine (2004). SOPs have been commonly observed in high latitudes, for example, as laminated structures of ozone with the highest frequency of occurrence during the spring season (Dobson, 1973). These laminated structures are primarily considered to be a winter-spring phenomenon, with a peak altitude of occurrence near 14 km (Reid and Vaughan, 1991). Varotsos et al. (1994) suggested that the north and northwest atmospheric circulations in the lower stratosphere play a key role in the formation of SOPs observed over Athens, Greece. Overall, the occurrence of SOPs is typically considered to be a northern hemispheric phenomenon, with no SOPs reported in the tropics and the southern hemisphere (Lemoine, 2004). Trickl et al. (2011) showed the influences of ozone import from the stratosphere and transport along the subtropical jet stream over Europe. According to the aforementioned studies, SOPs are mainly attributed to dynamical processes involving STE, advection and Rossby wave breaking events.

Recent studies (Hwang et al., 2005, 2007; Park et al., 2012) focusing on the Korean region showed that SOP events regularly occur over mid-latitudes. In contrast to earlier studies presenting SOPs mostly in the lower stratosphere, several SOPs were observed in the upper troposphere over Korea. Hwang et al. (2005) attributed these SOPs to the downward transport of ozone from the stratosphere within a timescale of about one day (24 h), typical of the cross-tropopause exchange. Furthermore, the frequency of occurrence, estimated from 9 years of ozonesonde observations, was found to have strong seasonal variability over Korea with a broad winter-spring maxima and frequencies of occurrence up to 50–80 % (Hwang et al., 2005). Moreover, Hwang et al. (2005) reported an increase in

Atmos. Chem. Phys. Discuss., doi:10.5194/acp-2016-908, 2016
Manuscript under review for journal Atmos. Chem. Phys.
Published: 2 November 2016

Atmospheric Chemistry and Physics Discussions

SOP occurrences over Korea, while the STT effects are anticipated to increase tropospheric ozone in the future (Banerjee et al., 2016).

The studies pertaining to the influences of STT on the vertical profiles of ozone are relatively sparse over the tropical Indian region. Mandal et al. (1998) analyzed observations from ozonesondes and an MST Radar, and attributed the enhanced ozone mixing ratios in the upper troposphere to STT through the indistinct tropopause over southern India. Fadnavis et al. (2010) combined satellite-borne measurements (TES and MLS) with simulations performed by the MOZART model and showed significant influences of STT over India in particular during winter and spring /pre-monsoon seasons. Venkat Ratnam et al. (2016) used satellite observations to estimate the effect of STE associated with tropical cyclones over the north Indian Ocean. Most of the studies based on in situ measurements have however been confined over the southern part of India (e.g. Mandal et al., 1998; Sinha et al., 2016) and the adjacent marine regions (Lal et al., 2013). Ganguly and Tzanis (2011) used ozonesonde observations from three Indian stations operated by the Indian Meteorological Department (IMD) and suggested that overall STT only plays a minor role into the budget of tropospheric ozone over India. However, the influences of STT were found to increase with latitude /northward over India (Ganguly and Tzanis, 2011).

Studies investigating the SOP structures and implications have been few over the tropical Indian region, until very recently (Ojha et al., 2014; Das et al., 2016). The events over southern India were found to be mainly associated with stratospheric intrusions during tropical cyclonic storms (Das et al., 2016). In contrast, the SOP events observed over the central Himalayas in northern India appear similar to what is typically observed over the mid-high latitudes as mentioned earlier. Moreover, SOPs were observed to be more frequent during spring, and were attributed to the combined effects of STE and advection (Ojha et al., 2014). In the previous work using weekly ozonesonde measurements (3–4 profiles per month), covering the period January 2011–December 2011 (Ojha et al., 2014), only 6 SOP events were observed, being insufficient to calculate the frequency and seasonality of SOP occurrences. Additionally, model simulations are required to both trace the source regions and quantify the effect of SOPs on the tropospheric ozone budget. Such investigation is of critical importance over central Himalayas, as satellite-based studies show high pollution loading over the northern India and the nearby Indo-Gangetic Plain (IGP) including the Tropospheric Column Ozone (TCO) over South Asia (Fishman et al., 2003).

In the present study, the global atmospheric chemistry climate model EMAC (ECHAM5/MESSy Atmospheric Chemistry) has been used to explore the processes causing the SOPs, investigate the frequency and seasonality of their occurrence and finally assess their impact on the tropospheric ozone budget over the central Himalayas.

Atmos. Chem. Phys. Discuss., doi:10.5194/acp-2016-908, 2016
Manuscript under review for journal Atmos. Chem. Phys.
Published: 2 November 2016

Atmospheric Chemistry and Physics Discussions

2 Methodology

2.1 EMAC

The ECHAM5/MESSy Atmospheric Chemistry (EMAC) is a numerical system for the simulation of regional and global air quality and climate (Jöckel et al., 2010). In this work the model results from simulation RC1SD-base-10a of the ESCiMo project (Jöckel et al., 2016) are used. The general circulation model ECHAM5 version 5.3.02 (Roeckner et al., 2006) and the Modular Earth Submodel System (MESSy) version 2.51 (Jöckel et al., 2016) were used at T42L90MA-resolution, implying a spherical truncation of T42 (corresponding to a quadratic Gaussian grid of approx. 2.8 by 2.8 degrees in latitude and longitude) and 90 vertical hybrid pressure levels up to 0.01 hPa. The dynamics of the general circulation model were weakly nudged by Newtonian relaxation towards ERA-Interim reanalysis data (Dee et al., 2011). Gas-phase and particulate trace species calculated with the EMAC model have been extensively evaluated in previous studies (e.g. Pozzer et al., 2007, 2010, 2012). Simulation RC1SD-base-10a was selected between the ESCiMo simulations as suggested in Jöckel et al. (2016) ("For intercomparison with observations, we recommend to use the results of [...] RC1SD-base-10a."). Detailed information on the model set-up and comparison with observations can be found in Jöckel et al. (2016).

A tracer of stratospheric ozone, denoted as O_3s in EMAC, has been used to quantify the effects of STT. O_3s follows the transport and destruction processes of ozone in the troposphere but not its chemical formation (Roelofs and Lelieveld, 1997) and it is initialized to O_3 in the stratosphere.

2.2 Tropopause height and tropopause folds

The Lapse Rate Tropopause (LRT) height is calculated from EMAC output using the WMO definition as the altitude at which lapse rate decreases to a value of 2 °C/km or less, provided that the average lapse rate between this level and all higher levels within the adjacent 2 km do not exceed 2 °C/km.

Tropopause folds in EMAC simulations were identified with an algorithm developed by Sprenger et al. (2003), and improved by Ŝkerlak et al. (2014), using the three dimensional fields of potential vorticity, potential temperature and specific humidity. The vertical extent of the folds, as determined by the difference between the upper and middle tropopause crossings (see Fig. 1 in Tyrlis et al. (2014)) has been further used to identify shallow, medium and deep folds, as described and used elsewhere (Tyrlis et al., 2014; Ŝkerlak et al., 2015; Akritidis et al., 2016).

2.3 Observational dataset

The occurrence of SOPs was reported using ozonesonde observations from Nainital (79.45° E, 29.37° N, 1958 m asl), a high altitude station located in the central Himalayan region (Ojha et al., 2014). These data have been used to evaluate the capability of EMAC to reproduce SOPs over this

Atmos. Chem. Phys. Discuss., doi:10.5194/acp-2016-908, 2016
Manuscript under review for journal Atmos. Chem. Phys.
Published: 2 November 2016

Atmospheric Chemistry and Physics Discussions

region. A typical event of SOP occurrence at Nainital observed on 10th March 2011 is shown in Fig. 1a. The ozone mixing ratios in the middle-troposphere (10–11 km) are clearly observed to be very high (150–250 nmol mol^{-1}) forming an SOP. The location of Nainital station and the geographical topography of the northern Indian region are also shown in Fig. 1b.

Ozone profiles at Nainital were measured using Electrochemical Concentration Cell (ECC) ozonesondes. The method utilizes the titration of ozone in potassium iodide solution, which leads to production of Iodine (I_2). The conversion of I_2 to I^- in the cell leads to the flow of two electrons for each ozone molecule entered. The measured cell current, flow rate of air along with sensor parameters, e.g. the background current and pump temperature, are used to derive ozone mixing ratios (Ojha et al., 2014). The precision and accuracy of ECC-ozonesondes are reported to be $\pm$(3–5)% and $\pm$(5–10)% respectively, up to 30 km altitude (Smit et al., 2007).

Further details of the Nainital station and meteorology (Sarangi et al., 2014; Singh et al., 2016) and balloon-borne measurements (Smit et al., 2007; Ojha et al., 2014; Naja et al., 2016) can be found elsewhere.

2.4 Backward trajectories

We used the Hybrid Single Particle Lagrangian Integrated Trajectory (HYSPLIT) model (http://ready.arl.noaa.gov/HYSPLIT.php) to investigate the source regions and the transport patterns causing SOPs over the central Himalayas. Backward trajectories have been simulated at 10, 11 and 12 km above sea level (asl), which are the typical altitudes where SOPs are observed in this study. HYSPLIT trajectory simulations are driven by NCEP reanalysis meteorological fields and the model vertical velocity option has been used for the vertical motions. More details of the backward trajectory simulations using the HYSPLIT model (Draxler and Hess, 1997, 1998; Draxler et al., 2014) and use of various datasets as meteorological inputs over the Indian region can be found elsewhere (e.g. Ojha et al., 2012; Kumar et al., 2015).

3 Results and Discussion

3.1 Model Evaluation

Fig. 2 shows the comparison of EMAC simulated ozone profiles with ozonesonde measurements over Nainital during six SOP events reported previously (Ojha et al., 2014). Model ozone fields have been bilinearly interpolated to the observation site and model output closer to the time of observation is weighted higher. As the vertical resolution of EMAC simulations is about 500–600 m in the middle troposphere (10–12 km), where SOPs are typically observed, the observational values are also shown at similar vertical resolution for comparison. The average ozone mixing ratios along with the corresponding standard deviations for the six events are compared between model and observations in Table 1 for lower, middle and upper tropospheric altitudes.

Atmos. Chem. Phys. Discuss., doi:10.5194/acp-2016-908, 2016
Manuscript under review for journal Atmos. Chem. Phys.
Published: 2 November 2016

Atmospheric Chemistry and Physics Discussions

The EMAC model is found capable of reproducing the altitudinal placement of the SOPs over the central Himalayas during all six events. For example, on 20th Apr and 9th May the model shows the peak ozone mixing ratios at 10.5 km asl, in agreement with the ozonesonde profiles. On other events, such as on 11th Feb, 10th Mar and 25th Oct, the altitude of SOP differs slightly (by 0.5-1 km) between model and ozonesonde profiles, except on 7th Jun (by 2 km). The aforementioned discrepancies in the altitude of SOPs occurrence might be related to the model vertical resolution.

In addition to the altitude of SOPs occurrence, EMAC also quantitatively captures the ozone enhancements. The model bias in simulating peak ozone mixing ratios is found to be varying from about -45 nmol mol^{-1} (7th Jun) to +34 nmol mol^{-1} (9th May). The biases are found to be within the variability of 1 standard deviation in 10–12 km altitude (28–59 nmol mol^{-1}) as calculated from ozonesonde observations during spring over this site (See Table 1 and Ojha et al. (2014)).

However, the model generally overestimates the ozone mixing ratios in the lower troposphere by about 11–24 nmol mol^{-1} (Table 1) and shows some limitation in capturing less pronounced SOPs, typically observed outside the winter-spring seasons. The bias in the absolute ozone enhancement (-45 nmol mol^{-1}) as well as in the altitudinal placement of the SOP (by 2 km) are higher on 7th Jun. However, these events were identified visually (Ojha et al., 2014) and here we show all for completeness. The SOP events will be selected based on specific criteria in order to calculate the frequency of occurrence, as discussed in detail in Sect. 3.3.

Possible biases between model and observations could arise from a variety of sources, most importantly, the time-evolution of the SOPs (Supplementary material - Figure 1). Therefore, the limited number of ozone profile measurements could lead to a temporal difference in the state of SOP evolution being compared between model and observation. We tried to minimize this effect by applying a weighted average algorithm, as mentioned above.

Overall, because the model is able to reproduce the occurrences of SOPs, their altitudinal placements and the ozone enhancements over the central Himalayas, we use EMAC simulations to investigate the underlying processes (Section 3.2), the frequency of occurrences (Section 3.3) and the effects on tropospheric ozone budget (Section 3.4).

3.2 Origin of SOPs

In this section, we analyze the EMAC simulated meteorological and chemical fields in conjunction with backward air trajectories to investigate the origin of SOPs over the central Himalayas. Fig. 3 shows the vertical profiles of potential vorticity (PV), a tracer of stratospheric intrusions, during the SOP events observed over Nainital. PV vertical profiles during all SOPs show layers of high values coinciding with the altitude of SOPs.

The enhanced PV layers are found to be weaker during June and October as compared to events during late winter and spring. PV values are found to be between 3.1 PVU (20th Apr) to 4.7 PVU (11th Feb) at the SOP altitudes for the events occurring in winter-spring. Even during the less pro-

Atmos. Chem. Phys. Discuss., doi:10.5194/acp-2016-908, 2016
Manuscript under review for journal Atmos. Chem. Phys.
Published: 2 November 2016

Atmospheric Chemistry and Physics Discussions

nounced events of early-summer and autumn, the PV values at SOP altitude are 1.8–2.5 PVU. The PV values at the SOP altitudes suggest that the air masses showing very high ozone levels (SOPs) are of stratospheric origin.

To quantify the amount of ozone transported from the stratosphere during the SOPs, we compare the EMAC simulated vertical profiles of O_3 with O_3s (Fig. 4). The model shows that nearly all excess ozone at the SOP altitudes is of stratospheric origin, during the winter and spring, despite of the fact that the SOPs are below the LRT, except on 10th Mar. Since the LRT over this region is located significantly higher (Fig. 4, also see Naja et al. (2016)) than the altitude of SOPs, and that the ozone in SOPs is found to be of stratospheric origin, we conclude that stratospheric air masses are sandwiched between tropospheric layers at 10–11 km altitude. This result complements previous studies primarily showing the altitudinal placement of SOPs at about 14 km near the Lower Stratosphere (UTLS) (e.g. Reid and Vaughan, 1991; Hwang et al., 2007).

The contribution of tropospheric photochemical sources to the SOPs can be represented by the difference O_3-O_3s, which is found to be large (about 50 nmol mol^{-1}), near SOP altitude on 7th Jun. This could be a combined effect of deep convective mixing towards the onset of the summer monsoon and weak horizontal winds (Ojha et al., 2014; Naja et al., 2016) leading to the accumulation of the photochemically processed air masses of tropospheric origin.

In order to investigate the underlying dynamics that transport the stratospheric air masses, leading to the SOPs over the Himalayas, we analyzed the backward air trajectories (Fig. 5), initialized over Nainital at 10, 11 and 12 km, which are the typical altitudes of the SOPs (Fig. 2). The air mass trajectories indicate rapid transport from the west, for example on 11th Feb, taking only two days for the air masses to be transported across Africa and Middle-East and reach the Himalayas (Fig. 5). Further, the locations of the tropopause folds occurred during the period of air trajectories are also shown. The tropopause folds are mostly found in a belt between about 20 and 35^{o}N, in agreement with previous studies (Ŝkerlak et al., 2015). The air masses have been encountering extensive tropopause dynamics along the path of transport, before reaching the Himalayas.

EMAC simulated O_3 vertical profiles along with the 5-day backward air trajectories are shown in Fig. 6. The pressure variations of the air masses and tropopause along the trajectory are also shown. In agreement with the analysis of PV and O_3s, there is no apparent downward transport of airmass, as typically observed in altitude variations of the backward trajectories during many STT events (e.g. Ma et al., 2014; Sarangi et al., 2014). Strong variability in the altitude of the LRT along the path of the transport is seen, except for the event of 7th Jun. This variability in LRT appears to be associated with the tropopause folds as shown in Fig. 5. Several shallow tropopause folds are seen along the transport path, while deeper folds (medium) are only seen during 11th Feb and 9th May (also see Ŝkerlak et al. (2015)). Intrusion of a significant amount of O_3 due to tropopause folds over the Eastern Mediterranean and the Middle-East was shown by Akritidis et al. (2016). The combination of very strong winds associated with the subtropical jets (Fig. 5, (Ojha et al., 2014; Naja et al.,

Atmos. Chem. Phys. Discuss., doi:10.5194/acp-2016-908, 2016
Manuscript under review for journal Atmos. Chem. Phys.
Published: 2 November 2016

Atmospheric Chemistry and Physics Discussions

2016)) and this intense tropopause dynamics, enriching the troposphere with stratospheric ozone, leads to the formation of SOPs over the Himalayas. Transport of stratospheric air during the analysis period is not found on 7th Jun (Fig. 6), which explains the smaller ozone enhancement in this event, probably related to the presence of some residual influences from previous days (Fig. 5 and 6).

The transport of ozone rich air masses from the stratosphere towards the Himalayas can be seen more clearly in the longitude-pressure cross sections at 30^{o}N (Fig. 7), and latitude-pressure cross sections at 80^{o}E (Fig. 8) for all the events and the day before. Fig. 7 reveals three geographical regions viz. Northern Africa and Atlantic Ocean, Middle-East and northern South Asia, where the intrusions of stratospheric air masses can be identified. Blobs of air masses characterized by high PV values (> 2 PVU) are also seen. Additionally, Fig. 8 shows a strong disparity in the stratospheric influences at 80^{o}E, with effects of STT mostly confined at latitudes higher than 25^{o}N, and minimal over the Southern India. This result based on EMAC simulations is found to be in agreement with the study by Ganguly and Tzanis (2011) based on ozonesonde observations at three Indian stations.

3.3 Frequency of SOPs

The frequency of SOP occurrences was not estimated over Nainital from observations, due to the availability of only 3-4 profiles in each month, however a tendency of higher frequency during spring was noticed (3 events), as compared to other seasons (1 event per season) (Ojha et al., 2014). In this section, we use long-term EMAC simulations, conducted for a period of 15 years (2000–2014), to investigate the frequency of SOP occurrence and seasonality over the central Himalayas. Due to the variability in the SOP altitude as well as the absolute enhancements during the SOPs, general / unique criteria can not be defined. Therefore, we first select the ozone profiles in which Average Ozone Mixing Ratios (AOMR) at 10–12 km, a typical altitude of SOP occurrence, are significantly higher (at least by 50%) compared to average ozone in the lower troposphere. Additionally, to explicitly select only the profiles which are SOPs (and not a direct intrusion over the Himalayas) the additional criterion was applied that directly above the SOP the ozone mixing ratios are again lower (at least by 20%), so that selected profiles have a shape typical of SOPs, as shown in Fig. 2. These two conditions can be mathematically expressed as

$$\mathrm{AOMR}_{10\text{–}12\mathrm{km}} \geqslant 1.5 \text{ x } \mathrm{AOMR}_{0\text{–}6\mathrm{km}}$$

and

$$\mathrm{AOMR}_{12\text{–}14\mathrm{km}} \leqslant 0.8 \text{ x } \mathrm{AOMR}_{10\text{–}12\mathrm{km}}$$

Further, the factors 1.5 and 0.8 representing an enhancement by 50% and reduction by 20% were suitably varied, which confirmed the generality of the result (not shown). We calculated the frequencies of occurrence in percentage for each month during 2000–2014, and converted these to an average climatological seasonal cycle, with the year-to-year variation shown as standard deviation (1-sigma) (Fig. 9).

Atmos. Chem. Phys. Discuss., doi:10.5194/acp-2016-908, 2016
Manuscript under review for journal Atmos. Chem. Phys.
Published: 2 November 2016

Atmospheric Chemistry and Physics Discussions

The highest frequency of SOPs over the central Himalayas is found during the pre-monsoon season (MAM), followed by winter (DJF). The frequency of SOP occurrences over Nainital increases steadily from January (2.7%) to May (10.8%), and abruptly declines in June (1.2%). The model does not predict any SOPs during July–October. It should be noted that here we included only those events as SOPs, which show enhancements by at least 50%, therefore some events with smaller enhancements could be present during July–October. It is suggested that the more frequent stratospheric intrusions during spring, combined with the stronger horizontal advection, lead to more frequent SOP events. The effects of stronger cross-tropopause exchange and influx of the stratospheric air masses during spring and winter over the Himalayas and surrounding regions, such as southern parts of the Tibetan Plateau, have also been shown by Ŝkerlak et al. (2014, 2015). The frequency of SOP events over this region is minimum during the summer monsoon season, as the weak horizontal winds (Ojha et al., 2014; Naja et al., 2016) do not transport the ozone from STTs over large distances. The frequency of stratospheric intrusions and tropopause folds over the Himalayas and surrounding regions are lower during the summer monsoon (Cristofanelli et al., 2010; Putero et al., 2016). Multiple tropopauses that can occur in winter and spring over the Tibetan Plateau are shown to be absent during the summer monsoon season (Chen et al., 2011). Additionally, stronger vertical mixing due to monsoonal convection inhibits high ozone layers to form and sustain. These findings are in agreement with the ground-based ozone measurements in the southern Himalaya, where about 78% of the stratospheric influences were attributed to the PV structures and subtropical jet streams, while monsoon depressions only account for 3% of the events (Bracci et al., 2012). Further, the seasonality of SOP frequency derived from EMAC simulations is consistent with the conclusions based on the limited number of observational profiles in Ojha et al. (2014). Next we determine the enhancements in tropospheric ozone columns due to presence of SOPs over the central Himalayas.

3.4 Effect of SOPs on Tropospheric Column Ozone

Fig. 10 shows the climatological mean seasonal cycle of the Tropospheric Column Ozone (TCO) in Dobson Units (DU) over Nainital from EMAC simulations over the period 2000–2014. TCO values are calculated by integrating ozone mixing ratios up to the LRT, determined using the WMO definition. To investigate the effect of SOPs on TCO, we compare three TCO values: First using EMAC simulated O_3 values from all time steps, second by selecting only the time steps when there is an SOP event as per the criteria discussed in Sec. 3.3, and third by taking all time steps when SOPs do not occur.

TCO values for All-times and No-SOPs are found to be very similar, mainly due to the large number of data counts (more than 1000 data counts in individual month), as compared to those in SOPs (0-120 data counts in individual month). The maxima of TCO during May and June (54.7±5.9 and 55.0±4.4 DU respectively) are attributed to the intense solar radiation and high pollution loading over northern India. While photochemical production of ozone is less efficient during the winter

Atmos. Chem. Phys. Discuss., doi:10.5194/acp-2016-908, 2016
Manuscript under review for journal Atmos. Chem. Phys.
Published: 2 November 2016

Atmospheric Chemistry and Physics Discussions

(TCO: 33.7±3.6 to 37.6±5.8 DU) and the summer monsoon (e.g. 44.9±4.9 DU in August). Overall, the EMAC simulated TCO seasonality from all data is found to be consistent with satellite data (Ojha et al., 2012) over this region.

The occurrences of SOPs are seen to clearly enhance the TCO values during the winter, pre-monsoon and early summer. The maximum enhancement in climatological average TCO value due to SOPs is found during January, when TCO values during SOPs (43.5±4.6 DU) are higher by as much as 9 DU (26%) compared to the non-SOP time steps (34.5±4.6 DU). The enhancements in tropospheric ozone loading over the central Himalayas due to SOPs are estimated to be 4–9 DU (7–26%) during January to June.

4 Conclusions

In this study, we used the EMAC model to investigate the layers of high ozone mixing ratios (SOPs) in the middle-upper troposphere, observed over the central Himalayas in northern India. EMAC successfully reproduces the occurrence, altitudinal placement and the relative ozone enhancements during SOP events observed in ozonesonde profiles. The vertical profiles calculated by EMAC show layers of high PV (1.8–4.7 PVU) coinciding with the altitude of SOPs suggesting the influences from stratospheric intrusions. The analysis of O_3s further shows that generally all excess ozone at SOP altitudes over the Himalayas is transported from the stratosphere. Photochemically produced (tropospheric) ozone is found to be significant only towards the onset of the summer monsoon.

Analysis of backward air trajectories in conjunction with EMAC simulated O_3 distributions and tropopause dynamics revealed that stratospheric air masses are sandwiched between tropospheric layers at 10–11 km altitude due to tropopause folds which are rapidly transported along the sub-tropical jet to cause SOP structures over the Himalayas. Regions as far as northern Africa and the Atlantic Ocean, the Middle-East and northern South Asia are found to be regions of stratospheric intrusions that act as sources of high-ozone mixing ratios. The distribution of O_3s showed that STT effects have been confined at latitudes higher than about 25°N and are minimal over the southern India.

We used long-term model simulations (2000–2014) to calculate the frequency of SOP occurrence showing maxima during spring (about 11% of the time in May), while no SOPs were predicted during the July–October months. This is consistent with results based on ozone soundings over the region. The high frequency of SOPs during spring is attributed to the occurrence of stratospheric intrusions combined with rapid horizontal transport. The minima in the frequency of SOPs during the summer monsoon are partially due to much weaker horizontal transport supplemented with stronger monsoonal convective mixing. Model simulations were further used to investigate the effect of SOPs on the TCO. The EMAC simulated TCO seasonality is in agreement with satellite data. SOP occurrence is found to significantly enhance the TCO over the region by 4–9 DU (7–26%).

Atmos. Chem. Phys. Discuss., doi:10.5194/acp-2016-908, 2016
Manuscript under review for journal Atmos. Chem. Phys.
Published: 2 November 2016

Atmospheric Chemistry and Physics Discussions

Acknowledgements. The model simulations have been performed at the German Climate Computing Centre (DKRZ) through support from the Bundesministerium für Bildung und Forschung (BMBF). DKRZ and its scientific steering committee are gratefully acknowledged for providing the HPC and data archiving resources for this consortial project ESCiMo (Earth System Chemistry integrated Modelling).

Atmos. Chem. Phys. Discuss., doi:10.5194/acp-2016-908, 2016
Manuscript under review for journal Atmos. Chem. Phys.
Published: 2 November 2016

Atmospheric Chemistry and Physics Discussions

344 **References**

345 Akritidis, D., Pozzer, A., Zanis, P., Tyrlis, E., Škerlak, B., Sprenger, M., and Lelieveld, J.: On the role
346 of tropopause folds in summertime tropospheric ozone over the eastern Mediterranean and the Mid-
347 dle East, Atmospheric Chemistry and Physics Discussions, 2016, 1–24, doi:10.5194/acp-2016-547, http:
348 //www.atmos-chem-phys-discuss.net/acp-2016-547/, 2016.
349 Banerjee, A., Maycock, A. C., Archibald, A. T., Abraham, N. L., Telford, P., Braesicke, P., and Pyle, J. A.:
350 Drivers of changes in stratospheric and tropospheric ozone between year 2000 and 2100, Atmospheric
351 Chemistry and Physics, 16, 2727–2746, doi:10.5194/acp-16-2727-2016, http://www.atmos-chem-phys.net/
352 16/2727/2016/, 2016.
353 Bracci, A., Cristofanelli, P., Sprenger, M., Bonafè, U., Calzolari, F., Duchi, R., Laj, P., Marinoni, A., Roccato,
354 F., Vuillermoz, E., and Bonasoni, P.: Transport of Stratospheric Air Masses to the Nepal Climate Observa-
355 tory–Pyramid (Himalaya; 5079 m MSL): A Synoptic-Scale Investigation, Journal of Applied Meteorology
356 and Climatology, 51, 1489–1507, doi:10.1175/JAMC-D-11-0154.1, 2012.
357 Chen, X. L., Ma, Y. M., Kelder, H., Su, Z., and Yang, K.: On the behaviour of the tropopause folding events over
358 the Tibetan Plateau, Atmospheric Chemistry and Physics, 11, 5113–5122, doi:10.5194/acp-11-5113-2011,
359 http://www.atmos-chem-phys.net/11/5113/2011/, 2011.
360 Cristofanelli, P., Bracci, A., Sprenger, M., Marinoni, A., Bonafè, U., Calzolari, F., Duchi, R., Laj, P., Pi-
361 chon, J. M., Roccato, F., Venzac, H., Vuillermoz, E., and Bonasoni, P.: Tropospheric ozone variations at
362 the Nepal Climate Observatory-Pyramid (Himalayas, 5079 m a.s.l.) and influence of deep stratospheric in-
363 trusion events, Atmospheric Chemistry and Physics, 10, 6537–6549, doi:10.5194/acp-10-6537-2010, http:
364 //www.atmos-chem-phys.net/10/6537/2010/, 2010.
365 Das, S. S., Ratnam, M. V., Uma, K. N., Subrahmanyam, K. V., Girach, I. A., Patra, A. K., Aneesh, S.,
366 Suneeth, K. V., Kumar, K. K., Kesarkar, A. P., Sijikumar, S., and Ramkumar, G.: Influence of tropical cy-
367 clones on tropospheric ozone: possible implications, Atmospheric Chemistry and Physics, 16, 4837–4847,
368 doi:10.5194/acp-16-4837-2016, http://www.atmos-chem-phys.net/16/4837/2016/, 2016.
369 Dee, D. P., Uppala, S. M., Simmons, A. J., Berrisford, P., Poli, P., Kobayashi, S., Andrae, U., Balmaseda,
370 M. A., Balsamo, G., Bauer, P., Bechtold, P., Beljaars, A. C. M., van de Berg, L., Bidlot, J., Bormann, N.,
371 Delsol, C., Dragani, R., Fuentes, M., Geer, A. J., Haimberger, L., Healy, S. B., Hersbach, H., Hólm, E. V.,
372 Isaksen, L., Kållberg, P., Köhler, M., Matricardi, M., McNally, A. P., Monge-Sanz, B. M., Morcrette, J.-
373 J., Park, B.-K., Peubey, C., de Rosnay, P., Tavolato, C., Thépaut, J.-N., and Vitart, F.: The ERA-Interim
374 reanalysis: configuration and performance of the data assimilation system, Quarterly Journal of the Royal
375 Meteorological Society, 137, 553–597, doi:10.1002/qj.828, http://dx.doi.org/10.1002/qj.828, 2011.
376 Dobson, G.: The laminated structure of the ozone in the atmosphere, Quarterly Journal of the Royal Meteoro-
377 logical Society, 99, 599–607, 1973.
378 Draxler, R. and Hess, G.: Description of the HYSPLIT 4 modeling system, NOAA Tech. Memo. ERL ARL-224,
379 NOAA Air Resources Laboratory, Silver Spring, MD, p. 24 pp., 1997.
380 Draxler, R. and Hess, G.: An overview of the HYSPLIT 4 modeling system of trajectories, dispersion, and
381 deposition, Aust. Meteor. Mag., 47, 295–308, 1998.
382 Draxler, R., Stunder, B., Rolph, G., Stein, A., and Taylor, A.: HYSPLIT4 USER's GUIDE, http://www.arl.noaa.
383 gov/documents/reports/hysplit_user_guide.pdf, 2014.

384 Fadnavis, S., Chakraborty, T., and Beig, G.: Seasonal stratospheric intrusion of ozone in the upper tropo-
385 sphere over India, Annales Geophysicae, 28, 2149–2159, doi:10.5194/angeo-28-2149-2010, http://www.
386 ann-geophys.net/28/2149/2010/, 2010.
387 Fishman, J., Wozniak, A. E., and Creilson, J. K.: Global distribution of tropospheric ozone from satellite mea-
388 surements using the empirically corrected tropospheric ozone residual technique: Identification of the re-
389 gional aspects of air pollution, Atmospheric Chemistry and Physics, 3, 893–907, doi:10.5194/acp-3-893-
390 2003, http://www.atmos-chem-phys.net/3/893/2003/, 2003.
391 Ganguly, N. D. and Tzanis, C.: Study of Stratosphere-troposphere exchange events of ozone in India and Greece
392 using ozonesonde ascents, Meteorological Applications, 18, 467–474, doi:10.1002/met.241, http://dx.doi.
393 org/10.1002/met.241, 2011.
394 Holton, J. R. and Lelieveld, J.: Stratosphere-Troposphere Exchange and its role in the budget of tropospheric
395 ozone, pp. 173–190, Springer Berlin Heidelberg, Berlin, Heidelberg, doi:10.1007/978-3-642-61051-6_8,
396 http://dx.doi.org/10.1007/978-3-642-61051-6_8, 1996.
397 Hwang, S.-H., Kim, J., Won, Y.-I., Cho, H. K., Kim, J. S., Lee, D.-H., Cho, G.-R., and Oh, S. N.: Sta-
398 tistical characteristics of secondary ozone density peak observed in Korea, Advances in Space Research,
399 36, 952–957, doi:http://dx.doi.org/10.1016/j.asr.2005.05.080, http://www.sciencedirect.com/science/article/
400 pii/S027311770500699X, 2005.
401 Hwang, S.-H., Kim, J., and Cho, G.-R.: Observation of secondary ozone peaks near the tropopause over the Ko-
402 rean peninsula associated with stratosphere-troposphere exchange, Journal of Geophysical Research: Atmo-
403 spheres, 112, n/a–n/a, doi:10.1029/2006JD007978, http://dx.doi.org/10.1029/2006JD007978, d16305, 2007.
404 Jöckel, P., Kerkweg, A., Pozzer, A., Sander, R., Tost, H., Riede, H., Baumgaertner, A., Gromov, S., and Kern, B.:
405 Development cycle 2 of the Modular Earth Submodel System (MESSy2), Geoscientific Model Development,
406 3, 717–752, doi:10.5194/gmd-3-717-2010, http://www.geosci-model-dev.net/3/717/2010/, 2010.
407 Jöckel, P., Tost, H., Pozzer, A., Kunze, M., Kirner, O., Brenninkmeijer, C. A. M., Brinkop, S., Cai, D. S.,
408 Dyroff, C., Eckstein, J., Frank, F., Garny, H., Gottschaldt, K.-D., Graf, P., Grewe, V., Kerkweg, A., Kern,
409 B., Matthes, S., Mertens, M., Meul, S., Neumaier, M., Nützel, M., Oberländer-Hayn, S., Ruhnke, R., Runde,
410 T., Sander, R., Scharffe, D., and Zahn, A.: Earth System Chemistry integrated Modelling (ESCiMo) with
411 the Modular Earth Submodel System (MESSy) versionÂ 2.51, Geoscientific Model Development, 9, 1153–
412 1200, doi:10.5194/gmd-9-1153-2016, http://www.geosci-model-dev.net/9/1153/2016/, 2016.
413 Kumar, A., Ram, K., and Ojha, N.: Variations in carbonaceous species at a high-altitude
414 site in western India: Role of synoptic scale transport, Atmospheric Environment, pp. –,
415 doi:http://dx.doi.org/10.1016/j.atmosenv.2015.07.039, http://www.sciencedirect.com/science/article/pii/
416 S1352231015302387, 2015.
417 Lacis, A. A., Wuebbles, D. J., and Logan, J. A.: Radiative forcing of climate by changes in
418 the vertical distribution of ozone, Journal of Geophysical Research: Atmospheres, 95, 9971–9981,
419 doi:10.1029/JD095iD07p09971, http://dx.doi.org/10.1029/JD095iD07p09971, 1990.
420 Lal, S., Venkataramani, S., Srivastava, S., Gupta, S., Mallik, C., Naja, M., Sarangi, T., Acharya, Y. B., and Liu,
421 X.: Transport effects on the vertical distribution of tropospheric ozone over the tropical marine regions sur-
422 rounding India, Journal of Geophysical Research: Atmospheres, 118, 1513–1524, doi:10.1002/jgrd.50180,
423 http://dx.doi.org/10.1002/jgrd.50180, 2013.

424 Lelieveld, J. and Dentener, F. J.: What controls tropospheric ozone?, Journal of Geophysical Research: Atmo-
425 spheres, 105, 3531–3551, doi:10.1029/1999JD901011, http://dx.doi.org/10.1029/1999JD901011, 2000.
426 Lemoine, R.: Secondary maxima in ozone profiles, Atmospheric Chemistry and Physics, 4, 1085–1096,
427 doi:10.5194/acp-4-1085-2004, http://www.atmos-chem-phys.net/4/1085/2004/, 2004.
428 Logan, J. A.: Tropospheric ozone: :Seasonal behavior, trends and antropogenic influence, J. Geophys. Res., 90,
429 10 463–10 482, 1985.
430 Logan, J. A.: Trends in the vertical distribution of ozone: an analysis of ozonesonde data, J. Geophys. Res., 99,
431 25 553–25 585, 1994.
432 Ma, J., Lin, W. L., Zheng, X. D., Xu, X. B., Li, Z., and Yang, L. L.: Influence of air mass downward
433 transport on the variability of surface ozone at Xianggelila Regional Atmosphere Background Station,
434 southwest China, Atmospheric Chemistry and Physics, 14, 5311–5325, doi:10.5194/acp-14-5311-2014,
435 http://www.atmos-chem-phys.net/14/5311/2014/, 2014.
436 Mandal, T. K., Cho, J. Y. N., Rao, P. B., Jain, A. R., Peshin, S. K., Srivastava, S. K., Bohra, A. K., and Mitra,
437 A. P.: Stratosphere-troposphere ozone exchange observed with the Indian MST radar and a simultaneous
438 balloon-borne ozonesonde, Radio Science, 33, 861–893, doi:10.1029/97RS03553, http://dx.doi.org/10.1029/
439 97RS03553, 1998.
440 Monks, P. S., Archibald, A. T., Colette, A., Cooper, O., Coyle, M., Derwent, R., Fowler, D., Granier, C., Law,
441 K. S., Mills, G. E., Stevenson, D. S., Tarasova, O., Thouret, V., von Schneidemesser, E., Sommariva, R., Wild,
442 O., and Williams, M. L.: Tropospheric ozone and its precursors from the urban to the global scale from air
443 quality to short-lived climate forcer, Atmospheric Chemistry and Physics, 15, 8889–8973, doi:10.5194/acp-
444 15-8889-2015, http://www.atmos-chem-phys.net/15/8889/2015/, 2015.
445 Myhre, G., Shindell, D., Breon, F.-M., Collins, W., Fuglestvedt, J., Huang, J., Koch, D., Lamarque, J.-F.,
446 Lee, D., Mendoza, B., Nakajima, T., Robock, A., Stephens, G., Takemura, T., and Zhang, H.: Anthro-
447 pogenic and Natural Radiative Forcing. In: Climate Change 2013: The Physical Science Basis. Contri-
448 bution of Working Group I to the Fifth Assessment Report of the Intergovernmental Panel on Climate
449 Change [Stocker, T.F., D. Qin, G.-K. Plattner, M. Tignor, S.K. Allen, J. Boschung, A. Nauels, Y. Xia, V.
450 Bex and P.M. Midgley (eds.)], Cambridge University Press, https://www.ipcc.ch/pdf/assessment-report/ar5/
451 wg1/WG1AR5_Chapter08_FINAL.pdf, 2013.
452 Naja, M., Bhardwaj, P., Singh, N., Kumar, P., Kumar, R., Ojha, N., Sagar, R., Satheesh, S. K., Krishna Moorthy,
453 K., and Kotamarthi, V. R.: High-frequency vertical profiling of meteorological parameters using AMF1 facil-
454 ity during RAWEX-GVAX at ARIES, Nainital, Curr. Sci., 110, 2317–2325, doi:10.18520/cs/v110/i12/2317-
455 2325, 2016.
456 Neu, J. L., Flury, T., Manney, G. L., Santee, M. L., Livesey, N. J., and Worden, J.: Tropospheric ozone
457 variations governed by changes in stratospheric circulation, NATURE GEOSCIENCE, 7, 340–344,
458 doi:10.1038/NGEO2138, 2014.
459 Ojha, N., Naja, M., Singh, K. P., Sarangi, T., Kumar, R., Lal, S., Lawrence, M. G., Butler, T. M., and
460 Chandola, H. C.: Variabilities in ozone at a semi-urban site in the Indo-Gangetic Plain region: Associa-
461 tion with the meteorology and regional processes, Journal of Geophysical Research: Atmospheres, 117,
462 doi:10.1029/2012JD017716, http://dx.doi.org/10.1029/2012JD017716, 2012.

463 Ojha, N., Naja, M., Sarangi, T., Kumar, R., Bhardwaj, P., Lal, S., Venkataramani, S., Sagar, R., Ku-
464 mar, A., and Chandola, H.: On the processes influencing the vertical distribution of ozone over
465 the central Himalayas: Analysis of yearlong ozonesonde observations, Atmospheric Environment,
466 88, 201–211, doi:http://dx.doi.org/10.1016/j.atmosenv.2014.01.031, http://www.sciencedirect.com/science/
467 article/pii/S1352231014000491, 2014.
468 Park, S. S., Kim, J., Cho, H. K., Lee, H., Lee, Y., and Miyagawa, K.: Sudden increase in the total ozone density
469 due to secondary ozone peaks and its effect on total ozone trends over Korea, Atmospheric Environment,
470 47, 226 – 235, doi:http://dx.doi.org/10.1016/j.atmosenv.2011.11.011, http://www.sciencedirect.com/science/
471 article/pii/S1352231011011745, 2012.
472 Pozzer, A., Jöckel, P., Tost, H., Sander, R., Ganzeveld, L., Kerkweg, A., and Lelieveld, J.: Simulating organic
473 species with the global atmospheric chemistry general circulation model ECHAM5/MESSy1: a comparison
474 of model results with observations, Atmospheric Chemistry and Physics, 7, 2527–2550, doi:10.5194/acp-7-
475 2527-2007, http://www.atmos-chem-phys.net/7/2527/2007/, 2007.
476 Pozzer, A., Pollmann, J., Taraborrelli, D., Jöckel, P., Helmig, D., Tans, P., Hueber, J., and Lelieveld, J.: Observed
477 and simulated global distribution and budget of atmospheric C_2–C_5 alkanes, Atmospheric Chemistry and
478 Physics, 10, 4403–4422, doi:10.5194/acp-10-4403-2010, http://www.atmos-chem-phys.net/10/4403/2010/,
479 2010.
480 Pozzer, A., de Meij, A., Pringle, K. J., Tost, H., Doering, U. M., van Aardenne, J., and Lelieveld, J.: Dis-
481 tributions and regional budgets of aerosols and their precursors simulated with the EMAC chemistry-
482 climate model, Atmospheric Chemistry and Physics, 12, 961–987, doi:10.5194/acp-12-961-2012, http:
483 //www.atmos-chem-phys.net/12/961/2012/, 2012.
484 Putero, D., Cristofanelli, P., Sprenger, M., Škerlak, B., Tositti, L., and Bonasoni, P.: STEFLUX, a tool for in-
485 vestigating stratospheric intrusions: application to two WMO/GAW global stations, Atmospheric Chemistry
486 and Physics Discussions, 2016, 1–23, doi:10.5194/acp-2016-514, http://www.atmos-chem-phys-discuss.net/
487 acp-2016-514/, 2016.
488 Reid, S. J. and Vaughan, G.: Lamination in ozone profiles in the lower stratosphere, Quarterly Journal of the
489 Royal Meteorological Society, 117, 825–844, 1991.
490 Roeckner, E., Brokopf, R., Esch, M., Giorgetta, M., Hagemann, S., Kornblueh, L., Manzini, E., Schlese, U., and
491 Schulzweida, U.: Sensitivity of Simulated Climate to Horizontal and Vertical Resolution in the ECHAM5
492 Atmosphere Model, Journal of Climate, 19, 3771–3791, doi:10.1175/JCLI3824.1, http://dx.doi.org/10.1175/
493 JCLI3824.1, 2006.
494 Roelofs, G.-J. and Lelieveld, J.: Model study of the influence of cross-tropopause O3 transports on tropo-
495 spheric O3 levels, Tellus B, 49, 38–55, doi:10.1034/j.1600-0889.49.issue1.3.x, http://dx.doi.org/10.1034/j.
496 1600-0889.49.issue1.3.x, 1997.
497 Sarangi, T., Naja, M., Ojha, N., Kumar, R., Lal, S., Venkataramani, S., Kumar, A., Sagar, R., and Chan-
498 dola, H. C.: First simultaneous measurements of ozone, CO, and NOy at a high-altitude regional repre-
499 sentative site in the central Himalayas, Journal of Geophysical Research: Atmospheres, 119, 1592–1611,
500 doi:10.1002/2013JD020631, http://dx.doi.org/10.1002/2013JD020631, 2014.
501 Shindell, D., Kuylenstierna, J. C. I., Vignati, E., van Dingenen, R., Amann, M., Klimont, Z., Anenberg, S. C.,
502 Muller, N., Janssens-Maenhout, G., Raes, F., Schwartz, J., Faluvegi, G., Pozzoli, L., Kupiainen, K., Höglund-

503 Isaksson, L., Emberson, L., Streets, D., Ramanathan, V., Hicks, K., Oanh, N. T. K., Milly, G., Williams, M.,
504 Demkine, V., and Fowler, D.: Simultaneously Mitigating Near-Term Climate Change and Improving Human
505 Health and Food Security, Science, 335, 183–189, doi:10.1126/science.1210026, http://science.sciencemag.
506 org/content/335/6065/183, 2012.
507 Singh, N., Solanki, R., Ojha, N., Janssen, R. H. H., Pozzer, A., and Dhaka, S. K.: Boundary layer evolu-
508 tion over the central Himalayas from Radio Wind Profiler and Model Simulations, Atmospheric Chemistry
509 and Physics Discussions, 2016, 1–33, doi:10.5194/acp-2016-101, http://www.atmos-chem-phys-discuss.net/
510 acp-2016-101/, 2016.
511 Sinha, P., Sahu, L., Manchanda, R., Sheel, V., Deushi, M., Kajino, M., Schultz, M., Nagendra, N., Kumar, P.,
512 Trivedi, D., Koli, S., Peshin, S., Swamy, Y., Tzanis, C., and Sreenivasan, S.: Transport of tropospheric and
513 stratospheric ozone over India: Balloon-borne observations and modeling analysis, Atmospheric Environ-
514 ment, 131, 228 – 242, doi:http://dx.doi.org/10.1016/j.atmosenv.2016.02.001, http://www.sciencedirect.com/
515 science/article/pii/S1352231016300905, 2016.
516 Ŝkerlak, B., Sprenger, M., and Wernli, H.: A global climatology of stratosphere-troposphere exchange us-
517 ing the ERA-Interim data set from 1979 to 2011, Atmospheric Chemistry and Physics, 14, 913–937,
518 doi:10.5194/acp-14-913-2014, http://www.atmos-chem-phys.net/14/913/2014/, 2014.
519 Ŝkerlak, B., Sprenger, M., Pfahl, S., Tyrlis, E., and Wernli, H.: Tropopause folds in ERA-Interim: Global clima-
520 tology and relation to extreme weather events, Journal of Geophysical Research: Atmospheres, 120, 4860–
521 4877, doi:10.1002/2014JD022787, http://dx.doi.org/10.1002/2014JD022787, 2014JD022787, 2015.
522 Smit, H. G. J., Straeter, W., Johnson, B. J., Oltmans, S. J., Davies, J., Tarasick, D. W., Hoegger, B., Stubi, R.,
523 Schmidlin, F. J., Northam, T., Thompson, A. M., Witte, J. C., Boyd, I., and Posny, F.: Assessment of the
524 performance of ECC-ozonesondes under quasi-flight conditions in the environmental simulation chamber:
525 Insights from the Juelich Ozone Sonde Intercomparison Experiment (JOSIE), Journal of Geophysical Re-
526 search: Atmospheres, 112, n/a–n/a, doi:10.1029/2006JD007308, http://dx.doi.org/10.1029/2006JD007308,
527 d19306, 2007.
528 Sprenger, M., Croci Maspoli, M., and Wernli, H.: Tropopause folds and cross-tropopause exchange: A global
529 investigation based upon ECMWF analyses for the time period March 2000 to February 2001, Journal of
530 Geophysical Research: Atmospheres, 108, n/a–n/a, doi:10.1029/2002JD002587, http://dx.doi.org/10.1029/
531 2002JD002587, 8518, 2003.
532 Tanimoto, H., Zbinden, R., Thouret, V., and Nédélec, P.: Consistency of tropospheric ozone observations made
533 by different platforms and techniques in the global databases, Tellus B, 67, http://www.tellusb.net/index.php/
534 tellusb/article/view/27073, 2015.
535 Trickl, T., Bärtsch-Ritter, N., Eisele, H., Furger, M., Mücke, R., Sprenger, M., and Stohl, A.: High-ozone layers
536 in the middle and upper troposphere above Central Europe: potential import from the stratosphere along the
537 subtropical jet stream, Atmospheric Chemistry and Physics, 11, 9343–9366, doi:10.5194/acp-11-9343-2011,
538 http://www.atmos-chem-phys.net/11/9343/2011/, 2011.
539 Tyrlis, E., Škerlak, B., Sprenger, M., Wernli, H., Zittis, G., and Lelieveld, J.: On the linkage between the Asian
540 summer monsoon and tropopause fold activity over the eastern Mediterranean and the Middle East, Journal
541 of Geophysical Research: Atmospheres, 119, 3202–3221, doi:10.1002/2013JD021113, http://dx.doi.org/10.
542 1002/2013JD021113, 2014.

Atmos. Chem. Phys. Discuss., doi:10.5194/acp-2016-908, 2016
Manuscript under review for journal Atmos. Chem. Phys.
Published: 2 November 2016

Atmospheric Chemistry and Physics Discussions

543 Varotsos, C., Kalabokas, P., and Chronopoulos, G.: Association of the Laminated Vertical Ozone Structure with
544 the Lower-Stratospheric Circulation, Journal of Applied Meteorology, 33, 473–476, 1994.
545 Venkat Ratnam, M., Ravindra Babu, S., Das, S. S., Basha, G., Krishnamurthy, B. V., and Venkateswararao, B.:
546 Effect of tropical cyclones on the stratosphere-troposphere exchange observed using satellite observations
547 over the north Indian Ocean, Atmospheric Chemistry and Physics, 16, 8581–8591, doi:10.5194/acp-16-8581-
548 2016, http://www.atmos-chem-phys.net/16/8581/2016/, 2016.

Table 1. A comparison of average ozone mixing ratios between ozonesondes and EMAC model for the lower, middle and upper troposphere during the six SOP events over Nainital

Date	2–7 km		7–12 km		12–17 km	
	Sonde	EMAC	Sonde	EMAC	Sonde	EMAC
20110211	50.7±4.1	69.5±3.6	85.8±52.1	112.3±52.3	135.9±22.9	173.7±42.6
20110310	67.6±8.1	86.8±1.8	120.5±52.0	134.8±39.0	131.9±57.4	184.7±76.9
20110420	85.8±7.7	96.9±7.0	147.1±37.3	136.8±28.6	151.4±41.6	151.0±36.7
20110509	83.0±13.3	101.6±5.3	104.8±34.7	154.8±25.3	132.9±15.4	140.7±17.7
20110607	83.1±7.6	107.0±6.1	132.4±30.2	110.2±10.0	119.8±21.6	111.9±35.2
20111025	57.1±3.3	72.3±1.7	84.4±26.8	86.7±17.2	123.3±37.6	130.4±31.7

Atmos. Chem. Phys. Discuss., doi:10.5194/acp-2016-908, 2016
Manuscript under review for journal Atmos. Chem. Phys.
Published: 2 November 2016

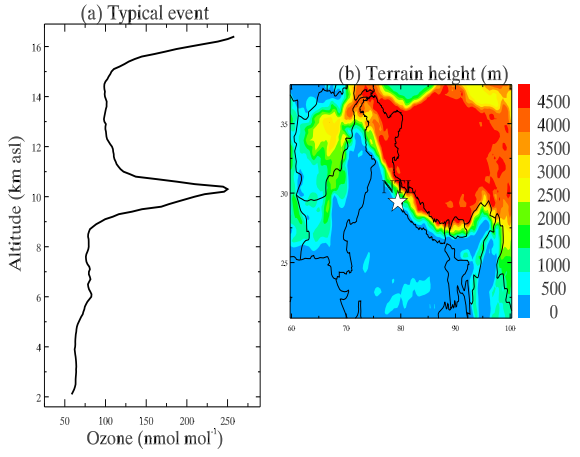

Figure 1. (a) A typical Secondary Ozone Peak (SOP) in an ozonesonde profile measured at 10–11 km altitude on 10th March 2011 over Nainital (Ojha et al., 2014). (b) Location of Nainital site in the central Himalayas shown in the topography map of the northern Indian region.

Atmos. Chem. Phys. Discuss., doi:10.5194/acp-2016-908, 2016
Manuscript under review for journal Atmos. Chem. Phys.
Published: 2 November 2016

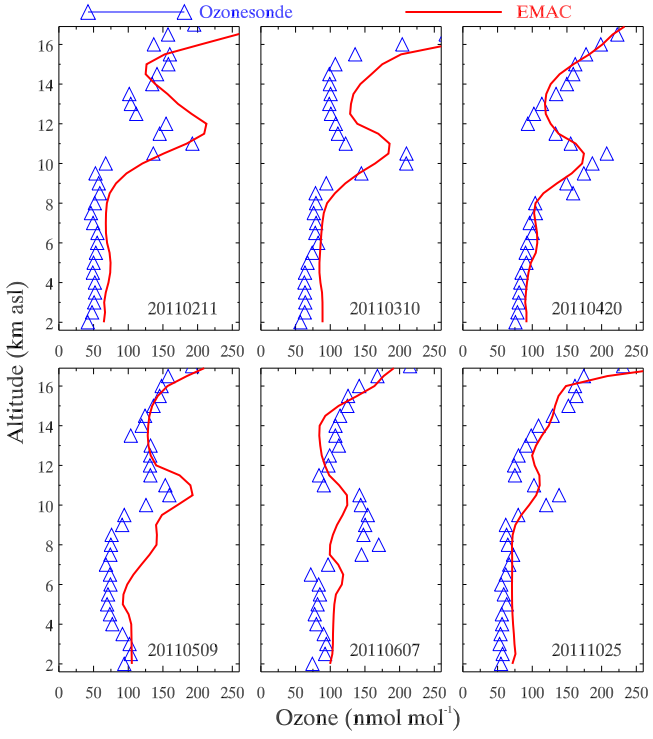

Figure 2. Comparison of EMAC simulated ozone profiles during the days of SOP events with ozonesonde observations over Nainital.

Atmos. Chem. Phys. Discuss., doi:10.5194/acp-2016-908, 2016
Manuscript under review for journal Atmos. Chem. Phys.
Published: 2 November 2016

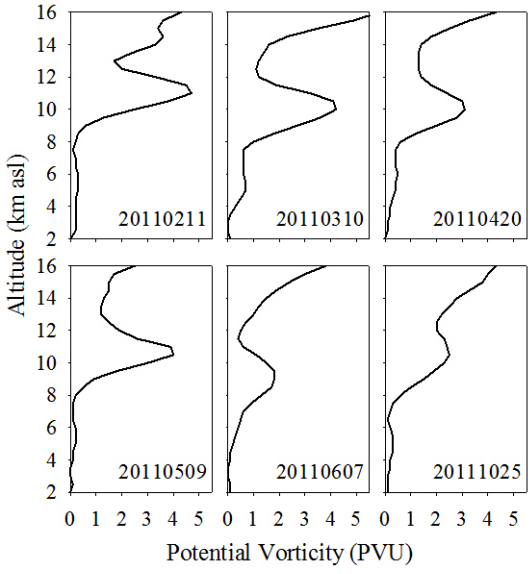

Figure 3. Vertical profiles of potential vorticity (PV) from EMAC simulations during the SOPs over Nainital.

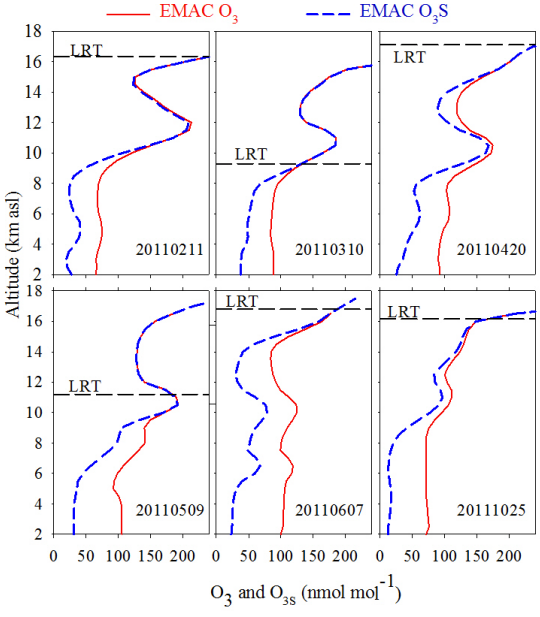

Figure 4. Vertical profiles of EMAC simulated ozone and stratospheric ozone tracer (O_{3S}) during the SOPs over Nainital. The height of the Lapse Rate Tropopause (LRT) from EMAC, calculated using the WMO definition, is also shown.

Atmos. Chem. Phys. Discuss., doi:10.5194/acp-2016-908, 2016
Manuscript under review for journal Atmos. Chem. Phys.
Published: 2 November 2016

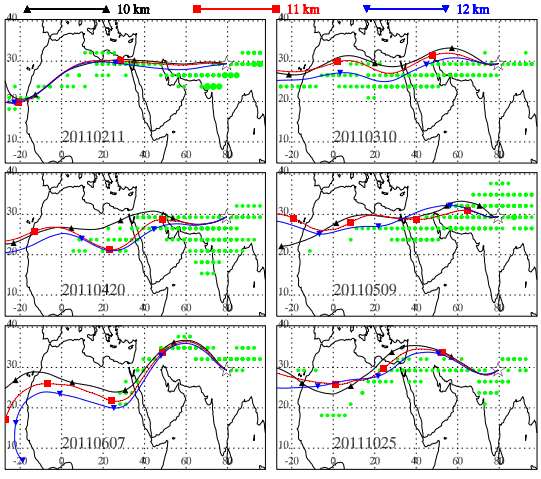

Figure 5. Backward air trajectories over Nainital for all events, with starting altitude of 10, 11 and 12 km. The difference between symbols on trajectories represent a time period of 1 day. The locations of tropopause folds 5 days prior to the event obtained from EMAC simulations are also shown. The location of Nainital site is shown by the star symbol. Small green circles represent shallow tropopause folds and bigger green circles (such as on 11thFeb) represent medium tropopause folds (see Sec. 3.2 for details).

Atmos. Chem. Phys. Discuss., doi:10.5194/acp-2016-908, 2016
Manuscript under review for journal Atmos. Chem. Phys.
Published: 2 November 2016

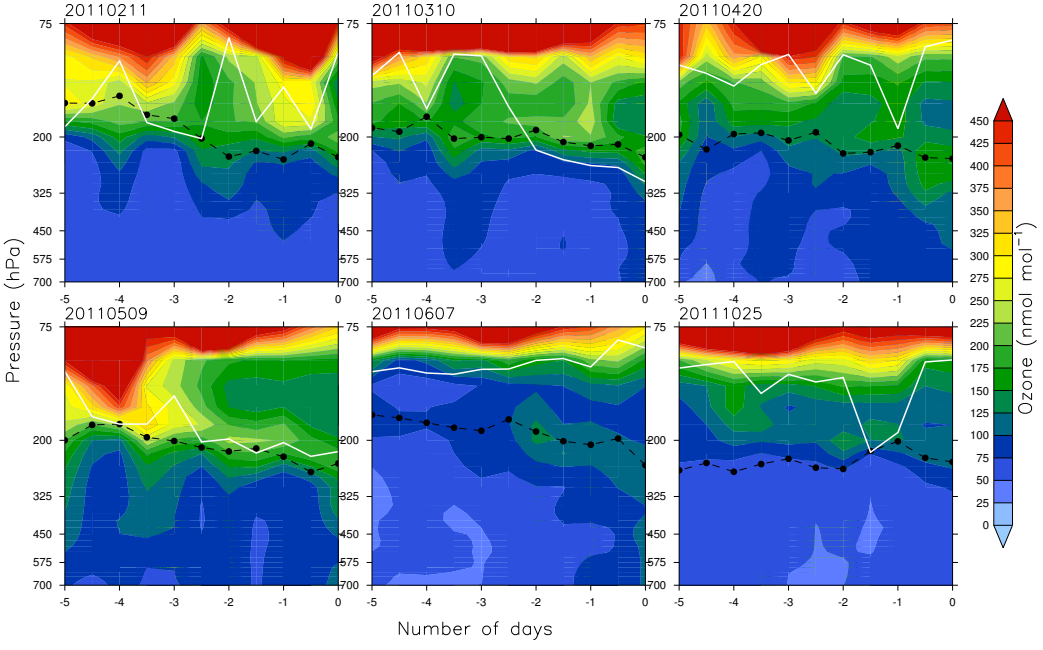

Figure 6. The vertical distribution of EMAC simulated O_3 along the trajectories with starting altitude of 11km over Nainital. The X axis shows the number of days back in time and the Y axis shows the pressure in hPa. The difference between two black circles here represents a time period of 12 h. The white line indicates the tropopause (LRT).

Atmos. Chem. Phys. Discuss., doi:10.5194/acp-2016-908, 2016
Manuscript under review for journal Atmos. Chem. Phys.
Published: 2 November 2016

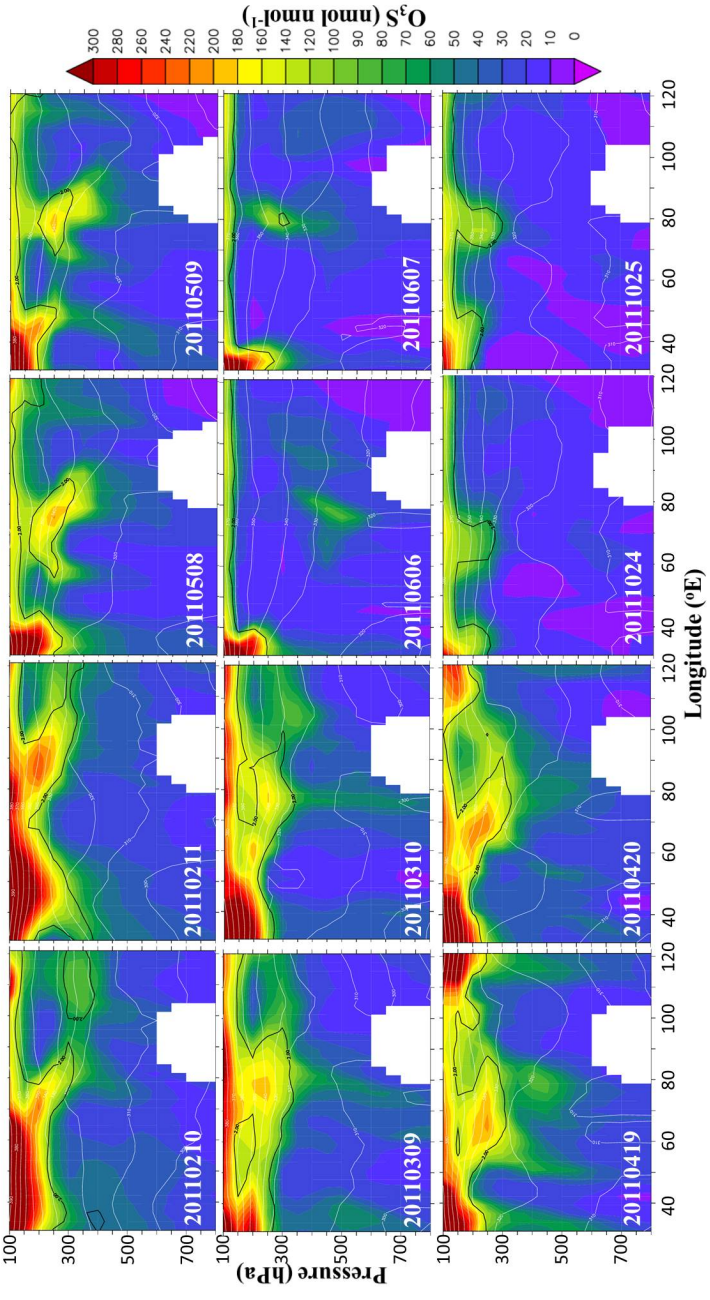

Figure 7. The longitude-pressure cross section of EMAC simulated O_3s during all SOP days and a day before the event. White lines denote the potential temperature (K) and the black line denotes the dynamical tropopause at 2 PVU.

Atmos. Chem. Phys. Discuss., doi:10.5194/acp-2016-908, 2016
Manuscript under review for journal Atmos. Chem. Phys.
Published: 2 November 2016

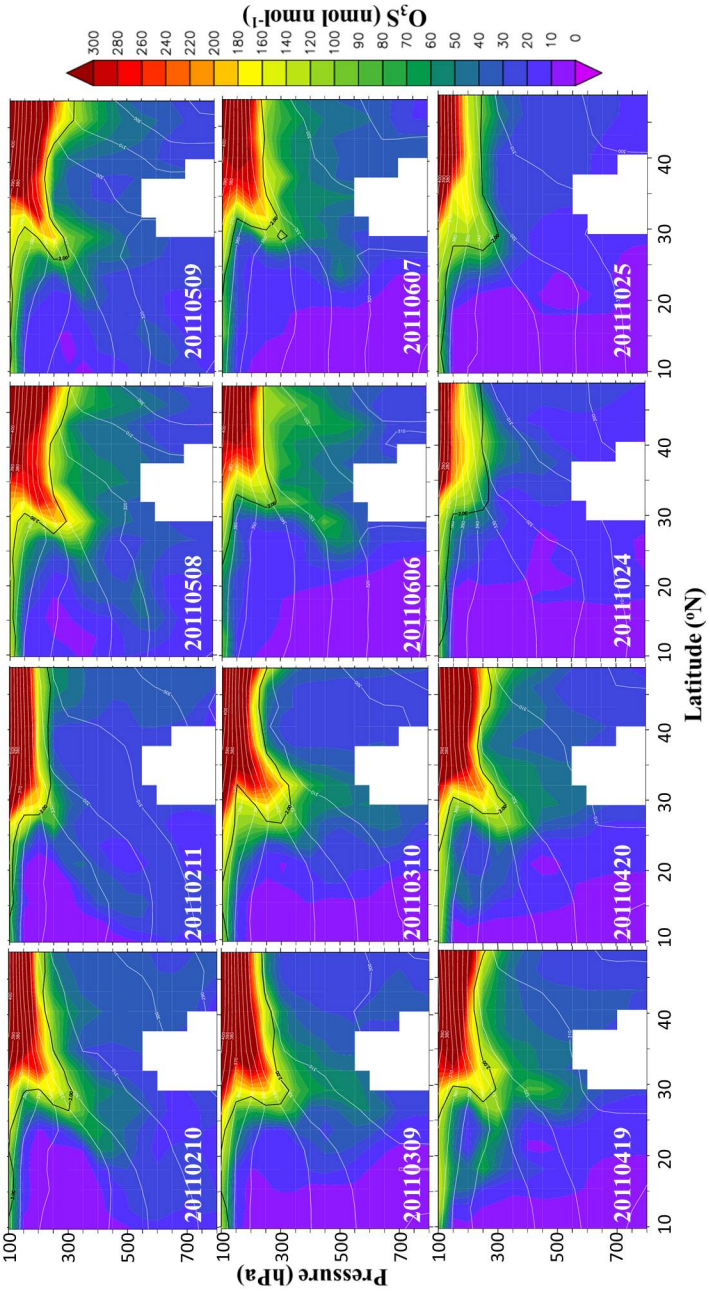

Figure 8. The latitude-pressure cross section of EMAC simulated O_3s during all SOP days and a day before the event. White lines denote the potential temperature (K) and the black line denotes the dynamical tropopause at 2 PVU.

Atmos. Chem. Phys. Discuss., doi:10.5194/acp-2016-908, 2016
Manuscript under review for journal Atmos. Chem. Phys.
Published: 2 November 2016

Atmospheric Chemistry and Physics Discussions

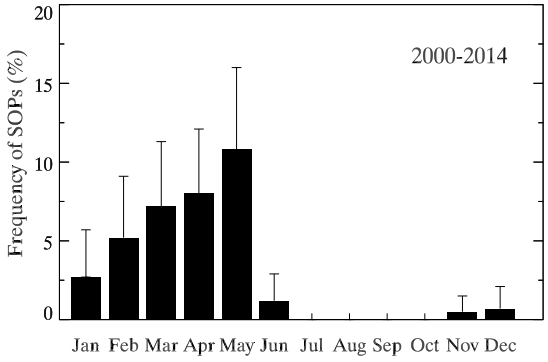

Figure 9. Annual cycle of SOPs occurrence frequency (%) over Nainital, calculated from the EMAC simulations for the period 2000–2014.

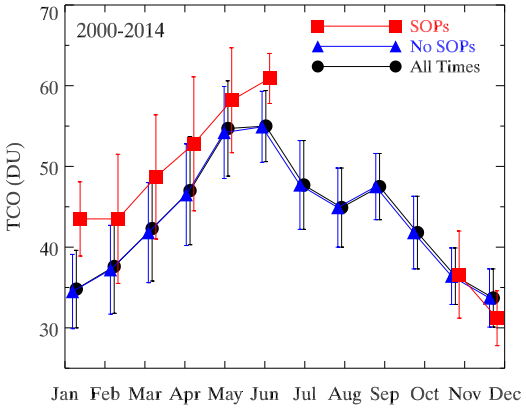

Figure 10. Annual cycle of EMAC simulated TCO over the central Himalayas calculated from 1) all EMAC time steps (All Times), 2) only the time steps having SOPs (SOPs), and 3) only when SOPs are not present (No SOPs) over the period 2000–2014.